








Article

Re-investigation of ‘minasgeraisite-(Y)’ from the Jaguarapu pegmatite, Brazil and high-temperature crystal chemistry of gadolinite-supergroup minerals

Oleg S. Vereshchagin^{1*} , Liudmila A. Gorelova¹ , Anastasia K. Shagova¹, Anatoly V. Kasatkin² , Radek Škoda³, Vladimir N. Bocharov⁴ , Natalia S. Vlasenko⁴  and Michaela Vašinová Galiová^{5,6}

¹Institute of Earth Sciences, Saint Petersburg State University, University Embankment 7/9, 199034 St. Petersburg, Russia; ²Fersman Mineralogical Museum of the Russian Academy of Sciences, Leninsky Prospect 18, 119071 Moscow, Russia; ³Department of Geological Sciences, Faculty of Science, Masaryk University, Kotlářská 2, CZ 611 37 Brno, Czech Republic; ⁴Geomodel Resource Center, Saint Petersburg State University, Ulyanovskaya Str. 1, 198504 St. Petersburg, Russia; ⁵Institute of Chemistry and Technology of Environmental Protection, Faculty of Chemistry, Brno University of Technology, Purkyňova 118, 61200 Brno, Czech Republic; and ⁶IC Brno, Purkyňova 125, 612 00, Brno, Czech Republic

Abstract

The chemical composition (including B, Be and Li), the Raman spectrum and the crystal-structure evolution (at the temperature range 27–1000°C) of a Mn-bearing, Bi-rich gadolinite-subgroup mineral from the Jaguarapu Pegmatite, Brazil (type-locality of minasgeraisite-(Y)) was studied. Elemental mapping revealed that the crystal investigated has complex chemical zonation with various Bi (~8–24 wt.% Bi₂O₃), Ca (~8–10 wt.% CaO) and Y (~11–17 wt.% Y₂O₃) content. The sample investigated has all the specific features of the chemical composition of minasgeraisite-(Y), except Ca excess and, thus, should be considered as hingganite-(Y). The Raman spectrum of the sample under study has bands at 140, 179, 243, 350, 446, 519, 559, 625, 902, 973, 3224, 3353, 3532 and 3763 cm⁻¹, and is similar to that of hingganite-(Y) / -(Nd). Crystal-structure refinement confirmed that the crystal in question should be considered as hingganite-(Y) and is in line with the previously obtained data on gadolinite-subgroup minerals from the Jaguarapu Pegmatite. High-temperature single-crystal X-ray diffraction studies revealed that the mineral starts to decompose above 800°C. We can conclude that beryllsilicates are most stable at high-temperature conditions within the gadolinite supergroup and that species with a higher *M*-site occupancy have higher stability upon heating.

Keywords: gadolinite, beryllsilicate, minasgeraisite-(Y), Raman, Jaguarapu Pegmatite, single-crystal X-ray diffraction, high temperature

(Received 28 November 2022; accepted 10 March 2023; Accepted Manuscript published online: 17 March 2023;
Associate Editor: G. Diego Gatta)

Introduction

The gadolinite-supergroup includes phosphates, beryllphosphates, beryllarsenates, borosilicates and beryllsilicates (Bačík *et al.*, 2017). Beryllsilicates are the most commonly found in Nature (e.g. Grew and Hazen, 2014), are most numerous within the supergroup (8 out of 14 minerals) and belong to the gadolinite subgroup (Bačík *et al.*, 2017). Gadolinite-subgroup minerals (‘gadolinites’) have the general chemical formula of A₂MBe₂Si₂O₈φ₂ (Bačík *et al.*, 2017), where A = Ca, rare earth elements [Y + lanthanides (*Ln*) = REE], Bi, etc.; M = Fe, vacancy, Mn, etc.; and φ = O, OH and F. The crystal structure of ‘gadolinites’ (space group *P*2₁/*c*) is usually described as alternating layers of tetrahedra (SiO₄ + BeO₄) with layers consisting of AO₆φ₂ tetragonal antiprisms and MO₄φ₂ octahedra. The tetrahedra form sheets with alternating four- and eight-membered rings, whereas the tetragonal

antiprisms and octahedra, connecting to each other, fill the inter-layer space (Foit and Gibbs, 1975; Bačík *et al.*, 2017). It is worth noting that according to the data available, the *A* site is always fully occupied, whereas the *M* site could be both occupied or vacant (Bačík *et al.*, 2017).

Natural ‘gadolinites’ are typically represented by a complex solid solution, which in most cases precludes unambiguous crystal structure refinement as up to 10 cations could be present at the *M* and/or *A* crystallographic site simultaneously (e.g. Demartin *et al.*, 1993; Cooper *et al.*, 2019). For this reason, a number of synthetic analogues of ‘gadolinites’ have been obtained; they contain REE, Mg, Mn, Ni, Co, Zn, Cu, Cd and Ga (e.g. Ito, 1965; 1966; 1967). Based on the data on natural and synthetic compounds, one can conclude that large cations (e.g. REE; *r*_i > 1 Å; Shannon, 1976) tend to occupy the *A* site in the crystal structure, whereas smaller cations (e.g. Fe²⁺, Mn²⁺, Mg; *r* < 1 Å; Shannon, 1976) occupy the *M* site only (Ito and Hafner, 1974; Foit and Gibbs, 1975). However, there is one exception: according to the Commission on New Minerals, Nomenclature and Classification (CNMNC) of the International Mineralogical Association (IMA), minasgeraisite-(Y) contains a relatively large Ca cation (*r* = 1 Å; Shannon, 1976) at the *M* site (Y₂CaBe₂Si₂O₈O₂; Foord *et al.*, 1986). As Foord *et al.* (1986) did

*Corresponding author: Oleg S. Vereshchagin; Email: o.vereshchagin@spbu.ru

Cite this article: Vereshchagin O.S., Gorelova L.A., Shagova A.K., Kasatkin A.V., Škoda R., Bocharov V.N., Vlasenko N.S. and Vašinová Galiová M. (2023) Re-investigation of ‘minasgeraisite-(Y)’ from the Jaguarapu pegmatite, Brazil and high-temperature crystal chemistry of gadolinite-supergroup minerals. *Mineralogical Magazine* 87, 470–479. <https://doi.org/10.1180/mgm.2023.19>

not conduct a detailed crystallographic investigation, Demartin *et al.* (2001) and Bačík *et al.* (2014, 2017) have questioned the very existence of minasgeraisite-(Y). Further, the mineral has not been reinvestigated since, which is partly due to its rarity (Cooper and Hawthorne, 2018).

Minasgeraisite-(Y) was discovered in the Jaguaraçu Pegmatite, Minas Gerais, Brazil (Foord *et al.*, 1986), and subsequently reported from the Krenn quarry, Matzersdorf/Tittling, Germany (Habel and Habel 2009), Vlastějovice region, Czech Republic (Novák *et al.* 2013) and Rigó Hill, Hungary (Zajzon *et al.*, 2015), but in neither case (except the type locality) does the reported composition correspond to the ideal minasgeraisite-(Y) end-member, and the structural data are not provided. According to Grew and Hazen (2014), minasgeraisite-(Y) could be considered as a mineral occurring only at the type locality.

Interestingly, there are two separate publications on Bi-rich 'gadolinite' from the Jaguaraçu Pegmatite: the first (Foord *et al.*, 1986) contains a description of minasgeraisite-(Y) (including inductively coupled plasma atomic emission spectroscopy data of the bulk sample and the unit cell parameters obtained by a Gandolfi camera) and the second (Cooper and Hawthorne, 2018) is devoted to the crystal-structure refinement of 'minasgeraisite-(Y)' (but no data on crystal chemistry are provided). Cooper and Hawthorne (2018) revealed the lowering of the symmetry (from $P2_1/c$ to $P1$) of 'minasgeraisite-(Y)' and showed no evidence of Ca at the M site. In addition, a discrepancy in the unit cell parameters calculated by Foord *et al.* (1986) and Cooper and Hawthorne (2018) was observed.

The high-temperature (HT) behaviour of 'gadolinites' could provide information on both their formation conditions (HT stability) and changes caused by the rising temperature (cation order / disorder and / or mineral recrystallisation). It has been shown previously that Th, U-rich metamict 'gadolinites' recrystallise under HT conditions, which makes the study of their crystal structure possible (e.g. Gibson and Ehlmann, 1970; Malczewski and Janeczek, 2002; Paulmann *et al.*, 2019). However, gadolinite-(Y) is the only 'gadolinite' which has been thoroughly studied in HT conditions (Paulmann *et al.*, 2019; Gorelova *et al.*, 2021a).

The sample used for the current study was given to us (A.V.K.) by Roy Kristiansen (Sellebakk, Norway), who, in turn, had obtained it from R.V. Gaines, the second author of the original article by Foord *et al.* (1986). However, following Cooper and Hawthorne (2018) we put minasgeraisite-(Y) in quotation marks, thus indicating that the material under investigation may not be minasgeraisite-(Y).

The aim of the current work was to (1) re-investigate 'minasgeraisite-(Y)' from the Jaguaraçu Pegmatite, Minas Gerais, Brazil (type locality) in order to obtain data on both the elemental composition and the crystal structure of the same crystal and (2) study the high-temperature crystal chemistry of 'minasgeraisite-(Y)' compared to closely related gadolinite-supergroup minerals.

Materials and methods

Two loose aggregates of 'minasgeraisite-(Y)' crystals from the Jaguaraçu Pegmatite, Minas Gerais, Brazil were used for the study. Optically they were euhedral, violet and transparent with an approximate size of <100 μm .

Raman spectra were collected from unpolished crystals using a LabRam HR 800 (Horiba Jobin-Yvon, Kyoto, Japan) spectrometer

equipped with a BX-41 (Olympus, Tokyo, Japan) microscope and a back-scattered geometry system in ambient conditions using a 532 nm laser. The confocal hole was 100 μm , and the 1800 gr/mm grating was used. The Raman spectra of the unoriented sample were recorded in the range of 70–4000 cm^{-1} at a resolution of 2 cm^{-1} and 30 s acquisition time. The laser power was focused on the point of size $\sim 2 \mu\text{m}^2$ by 100 \times objective. To improve the signal-to-noise ratio, the number of acquisitions was set to 5.

The single-crystal X-ray diffraction (SCXRD) analysis was performed using a Rigaku XtaLAB Synergy-S (Rigaku Oxford Diffraction, Japan) diffractometer equipped with a HyPix-6000HE detector with monochromated MoK α radiation (0.71073 Å) at 50 kV and 40 mA. More than a hemisphere of three-dimensional data was collected with the frame widths of 0.5–0.75°, depending on the temperature. For the experiments under ambient conditions, two single crystals with an approximate size of 40 $\mu\text{m} \times 40 \mu\text{m} \times 30 \mu\text{m}$ were mounted on a polymer loop using Paratone-N. Both crystals under investigation have similar quality and chemical composition (see below), so one of them was chosen for high-temperature studies. The thermal behaviour of the crystal under heating in air was studied *in situ* by high-temperature SCXRD using the same diffractometer equipped with a high-temperature FMB system (Oxford, UK). For these experiments, the same single crystal was mounted on the quartz glass fibre (for more details see Gorelova *et al.*, 2021a). SCXRD data were collected at different temperatures in the range of 27–1000°C with the temperature step 150°C below 600°C and 100°C above 600°C (there were 9 experimental points in total, including ambient temperature), temperature determination errors were $\pm 10^\circ\text{C}$ (see Gorelova *et al.*, 2022). The data were integrated and corrected for background, Lorentz, and polarisation effects. An empirical absorption correction based on the spherical harmonics implemented in the SCALE3 ABSPACK algorithm was applied in the *CrysAlisPRO* program (Agilent, 2012). The unit-cell parameters were refined using the least-square techniques. The *SHELXL* program package (Sheldrick, 2015) was used for all structural calculations. The calculation of the thermal-expansion parameters tensor and its visualisation was performed using the TTT program package (Bubnova *et al.*, 2013).

The elemental composition of the crystals used for SCXRD was analysed on the epoxy-mounted, polished, and carbon-coated sample by means of a scanning electron microscope (SEM), electron microprobe (EMP), and laser ablation system attached to an inductively coupled plasma-mass spectrometer (LA-ICP-MS). Energy-dispersive X-ray spectroscopy (EDS) analyses were performed on a S-3400 N (Hitachi, Japan) SEM equipped with an AzTec Energy XMax 20 (Oxford, UK) SSD detector with an accelerating voltage of 20 kV, beam current of 1 nA, and 1 μm beam diameter at the sample surface. EDS X-ray maps were obtained using 20 kV accelerating voltage, 1.5 nA beam current and 60 s dwell time.

The analyses in the wavelength-dispersive mode (WDS) were acquired by means of a SX-100 electron microprobe (Cameca, France) at 15 kV, 20 nA and 5 μm of beam diameter. The following natural and synthetic phases were employed for calibration: albite for Si, Al, wollastonite for Ca, fayalite for Fe, rhodonite for Mn, Mg₂SiO₄ for Mg, UO₂ for U, YAG for Y, lammerite for Cu, gahnite for Zn, Ca₅(PO₄)₃F for P, metallic Bi for Bi, and individual LnPO₄ for lanthanoids. Peak counting times (CT) were 20 s for major elements and 60 s for minor elements; CT for each background was one-half of the peak time. A thorough WDS angle scan was performed prior to the analysis to inspect

spectral interferences and guarantee the proper setting of the background positions. Spectral coincidences among lanthanides and other elements were corrected by empirically determined correction factors (see Škoda *et al.*, 2015 for details). Raw intensities were converted to concentrations using *X-PHI* (Merlet, 1994) matrix-correction software.

The Be, B and Li contents were determined using a LA-ICP-MS consisting of a quadrupole based ICP-MS (Agilent 7900) connected to an ArF⁺ excimer laser ablation system Analyte Excite+ (Teledyne CETAC Technologies). The laser ablation system emits a laser beam at a wavelength of 193 nm and is equipped with a 2-Volume Cell HelEx II. The ablated material was carried by He flow (0.5 and 0.31 min⁻¹) and mixed with Ar (~11 min⁻¹) prior to entering the ICP mass spectrometer. The sample surface of individual spots was ablated for 30 s per spot by a 25 μm laser beam diameter with the fluence of 5 J cm⁻², 10 Hz repetition rate and 60 s washout time. The monitored isotopes are as follows: ⁷Li⁺, ⁹Be⁺, ^{10,11}B⁺, ^{28,29}Si⁺, ^{43,44}Ca⁺ and ⁸⁹Y⁺.

The ICP-MS was tuned using a SRM NIST 612 with respect to the sensitivity and minimum doubly charged ions ($Ce^{2+}/Ce^{+} < 5\%$), oxide formation ($^{248}ThO^{+}/^{232}Th^{+} < 0.3\%$) and mass response $^{238}U^{+}/^{232}Th^{+} \sim 1$. The potential interferences were minimised *via* a collision cell (He 1 ml min⁻¹). The elemental contents were calibrated using artificial glass standards SRM NIST 610 and 612, and Si as the internal reference element after the baseline correction and the integration of the peak area using *HDIP* software (Teledyne CETAC Technologies, Omaha, Nebraska, USA). The accuracy of Be and B measurements was controlled using well-defined homogenous internal reference materials and the data obtained by SCXRD data (see above). As the data on light elements (Be, B and Li) were obtained, it was possible to calculate the chemical formulae assuming that the sum of tetrahedral cations (Be+B+Si+Al+P) equals 4 ($T+Q=4$). The number of (OH)-groups was charge balanced to keep the empirical formula electroneutral. As the content of Li₂O was low (~0.01 wt.%), Li was excluded from the empirical formula calculation.

Results and discussion

Composition of Bi-rich ‘gadolinites’ from the Jaguarçu Pegmatite

Back-scattered electron (BSE) photography showed that crystal aggregates are rosette-like; they are composed of separate platy crystals with a size 5–10 μm. Exceptionally, the size of the crystals exceeds 50 μm. These crystals are chemically heterogeneous in BSE images (Fig. 1a). The chemical analysis (EDS, WDS) and EDS mapping revealed that such chemical zonation is caused by the variable Bi (most prominent), Ca and Y (as a dominant REE) content (Fig. 1b–d). We have found an inverse correlation between Bi and Y ($n=13$, $r=-0.95$) and Bi and Ca ($n=13$, $r=-0.72$).

The WDS analysis of Bi-rich and Bi-poor zones of ‘minasgeraisite-(Y)’ from the Jaguarçu Pegmatite are shown in Table 1. Interestingly, our calculations (Table 1) prove that both zones of the crystal at hand belong to the same mineral species, namely hingganite-(Y) (Fig. 2). The *T* site is occupied exclusively by Si (Si > 2 atoms per formula unit (apfu); Table 1), the *Q* site is occupied mainly by Be (Be > 1.62 apfu), the *M* site is mostly vacant (the sum of *M* site cations < 0.33), the *A* site is occupied mainly by Y ($^{4}Ca/\text{sum of A site cations} < 0.39$) and the φ site is OH dominant (OH > 1.34).

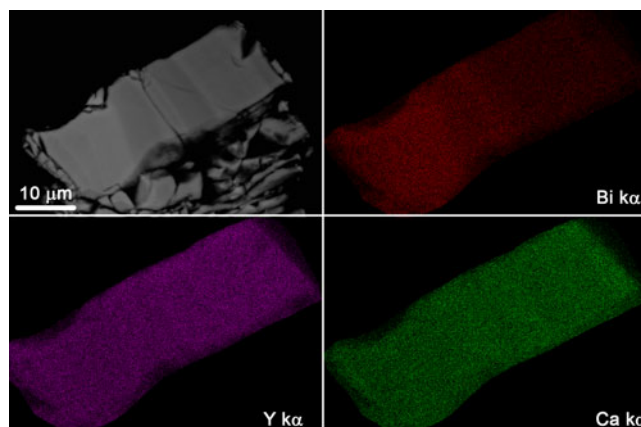


Figure 1. Chemical zonation in the studied crystal of ‘minasgeraisite-(Y)’: (a) back-scattered electron (BSE) image; (b) BiK α element-distribution map; (c) YK α element-distribution map; and (d) CaK α element-distribution map.

Generally, the sample under study has all the specific features of the composition of minasgeraisite-(Y) reported from the Jaguarçu Pegmatite, except Ca excess at the *M* site (Table 1). It has a high Bi (0.16–0.48 apfu) and Mn (0.19–0.21 apfu) content, which is typical for minasgeraisite-(Y) (Foord *et al.*, 1986) and has not been encountered in any other ‘gadolinite’ localities. It contains a relatively high content of Yb, Er, and Dy and has a very limited amount of lighter lanthanides, which is quite unique and resembles the REE-pattern (Fig. 3) of minasgeraisite-(Y) (Foord *et al.*, 1986) and ‘gadolinites’ from Kola peninsula (e.g. Belolipetsky *et al.*, 1968; Table 1). In addition, it has a very low Fe and Mg (both <0.1 apfu) content at the *M*-site, contains quite a small amount of B (<0.15 apfu) and almost no Li (~0.1 wt.% of Li₂O) at the *Q*-site, which is also in accordance with the data of Foord *et al.* (1986).

Raman spectra of ‘minasgeraisite-(Y)’ in comparison with other ‘gadolinites’

The Raman spectrum of ‘minasgeraisite-(Y)’ is shown on Fig. 4. The sample being investigated has a number of bands in the 100–1000 cm⁻¹ region (Fig. 5). The most intense are 140, 179, 243, 350, 446, 519, 559, 625, 902, 973, 3224, 3353, 3532 and 3763 cm⁻¹.

The Raman bands at 140, 179 and 243 cm⁻¹ are assigned to mixed lattice modes, 350 and 446 cm⁻¹ – stretching vibrations of the AO₄(OH)₂ tetragonal antiprisms and MO₄(OH)₂ octahedra, 519 and 559 cm⁻¹ – bending vibrations of the layer constituted by the SiO₄ and BeO₄ tetrahedra, 625 cm⁻¹ – Be–O stretching vibrations, 902 and 973 cm⁻¹ – Si–O stretching vibrations (Škoda *et al.*, 2018; Gorelova *et al.*, 2020; Kasatkin *et al.*, 2020). The bands at 3224, 3353, 3532 and 3763 cm⁻¹ are attributed to the stretching vibrations of (OH)-units. Prominent bands related to the (OH)-stretching vibrations are in a good agreement with the chemical formula calculations. No Raman bands were observed in the range from 1000 to 3200 cm⁻¹, which confirms the absence of CO₃²⁻ and H₂O groups.

The Raman spectrum of ‘minasgeraisite-(Y)’ has many similarities with the Raman spectra of other ‘gadolinites’ but is closer to hingganites (Table 2). Gadolinite-(Nd) (Škoda *et al.*, 2018) and -(Y) (Gorelova *et al.*, 2021a) have two intense Raman bands at ~900 and ~1000 cm⁻¹, whereas the Raman bands in the spectra

Table 1. Elemental composition and preliminary crystal-chemical formula for gadolinite-subgroup minerals from the Jaguaraçu pegmatite, Brazil (No 1–4) and Keivy pegmatite, Russia (No 5).

No.	1	2	3	4	5		1	2	3	4	5	
Ref.	Our data	Our data	Foord <i>et al.</i> (1986)		Belolipetsky <i>et al.</i> (1968)		Our data	Our data	Foord <i>et al.</i> (1986)		Belolipetsky <i>et al.</i> (1968)	
	Bi-rich zone	Bi-poor zone	Bi-rich zone	Bulk sample	Bulk sample		Bi-rich zone	Bi-poor zone	Bi-rich zone	Bulk sample	Bulk sample	
Wt.%												
CaO	7.89	9.80	8.10	11.47	2.64		0.67	0.78	0.54	0.58	0.38	
Bi ₂ O ₃	23.60	8.17	28.50	14.70	bdl		0.48	0.16	0.63	0.31	-	
Y ₂ O ₃	11.96	17.06	11.30	16.38	24.78		0.50	0.67	0.51	0.71	1.04	
La ₂ O ₃	0.25	0.11	0.20	0.25	bdl		0.01	-	0.01	0.01	-	
Ce ₂ O ₃	bdl	bdl	bdl	0.20	0.49		-	-	-	0.01	0.01	
Pr ₂ O ₃	0.11	bdl	0.10	0.15	bdl		-	-	-	-	-	
Nd ₂ O ₃	0.37	0.18	0.20	0.50	0.33		0.01	-	0.01	0.01	0.01	
Sm ₂ O ₃	0.24	0.22	0.10	0.26	0.33		0.01	0.01	-	0.01	0.01	
Eu ₂ O ₃	bdl	bdl	bdl	bdl	0.07		-	-	-	-	-	
Gd ₂ O ₃	0.30	0.42	0.20	0.32	0.54		0.01	0.01	0.01	0.01	0.01	
Tb ₂ O ₃	0.11	0.15	0.10	0.23	0.07		-	-	-	0.01	-	
Dy ₂ O ₃	1.17	1.61	1.30	1.26	4.50		0.03	0.04	0.04	0.03	0.11	
Ho ₂ O ₃	0.32	0.43	0.30	0.37	1.46		0.01	0.01	0.01	0.01	0.04	
Er ₂ O ₃	1.68	2.28	1.30	1.94	7.16		0.04	0.05	0.03	0.05	0.18	
Tm ₂ O ₃	0.60	0.71	0.60	0.75	1.15		0.01	0.02	0.02	0.02	0.03	
Yb ₂ O ₃	6.45	8.25	5.90	7.86	6.43		0.16	0.19	0.15	0.19	0.15	
Lu ₂ O ₃	1.32	1.61	1.50	1.71	1.01		0.03	0.04	0.04	0.04	0.02	
FeO	0.17	0.21	0.70	0.69	9.79	<i>M</i> site						
Fe ₂ O ₃	-	-	-	-	1.27	Ca	-	-	0.20	0.41	-	
CuO	0.11	0.25	0.10	0.14	-	Mn	0.21	0.19	0.25	0.19	0.02	
ZnO	0.47	0.25	0.30	0.35	-	Mg	0.06	0.10	0.08	0.07	0.03	
MnO	3.18	2.97	3.50	2.83	0.29	Fe ²⁺	0.01	0.01	0.05	0.05	0.64	
MgO	0.50	0.94	0.60	0.61	0.25	Fe ³⁺	-	-	-	-	0.07	
SiO ₂	26.85	30.11	24.50	26.37	24.82	Cu	0.01	0.01	0.01	0.01	-	
Al ₂ O ₃	bdl	bdl	bdl	0.32	2.00	Zn	0.01	0.01	0.01	0.02	-	
P ₂ O ₅	bdl	bdl	1.20	1.21	-	<i>T+Q</i> sites						
BeO	9.05	9.15	7.80	7.80	9.13	Si	2.12	2.22	2.10	2.14	1.95	
B ₂ O ₃	1.02	1.08	1.45	1.45	-	Al	-	-	-	0.05	0.32	
H ₂ O	3.17	3.21	0.89	1.38	0.71	P	-	-	0.09	0.08	-	
Total	100.89	99.17	100.99	101.23	99.98	Be	1.74	1.62	1.60	1.52	1.73	
						B	0.14	0.15	0.21	0.20	-	
						φ						
						OH	1.68	1.59	0.78	0.48	0.47	
						O	0.32	0.41	1.22	1.52	1.53	
						Σ REE	0.83	1.04	0.83	1.11	1.61	
						^A Ca/sum of <i>A</i> -site cations	0.34	0.39	0.10	0.21	0.12	
						^T Si/sum of <i>T</i> -site cations	1.00	1.00	1.00	1.00	1.00	
						Σ <i>M</i> -site cations	0.32	0.33	0.61	0.76	0.83	

Note: bdl – below detection limit

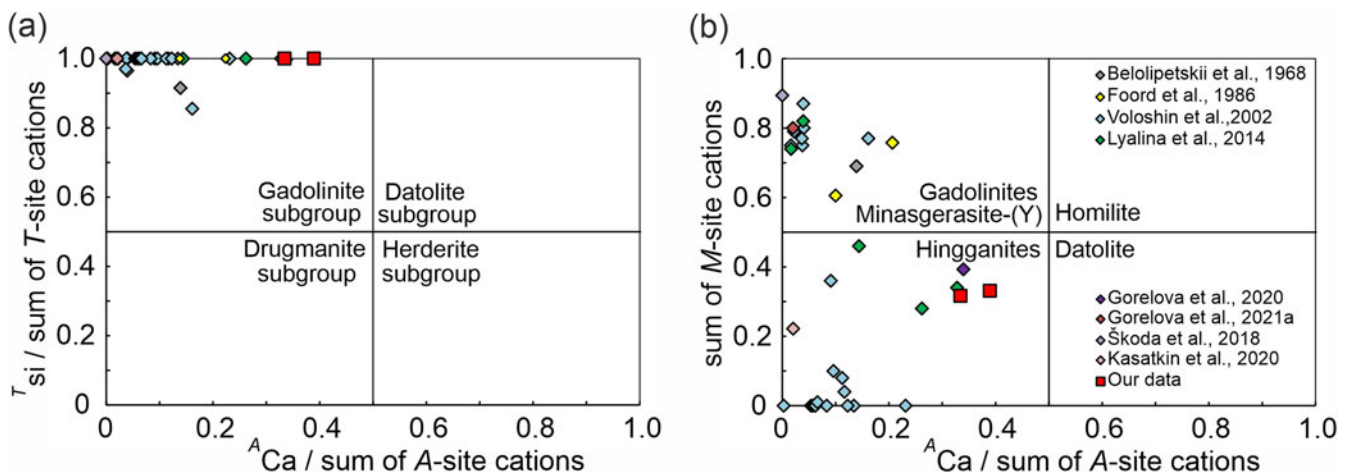


Figure 2. Selected data on gadolinite-subgroup minerals plotted on classification diagrams of the gadolinite supergroup: (a) for determination of groups and subgroups; and (b) for species determination. The legend for both graphs is given on the (b) graph. Refs: Belolipetsky *et al.* (1968); Foord *et al.* (1986); Gorelova *et al.* (2020), (2021a) Kasatkin *et al.* (2020); Lyalina *et al.* (2014); Škoda *et al.* (2018); Voloshin *et al.* (2002).

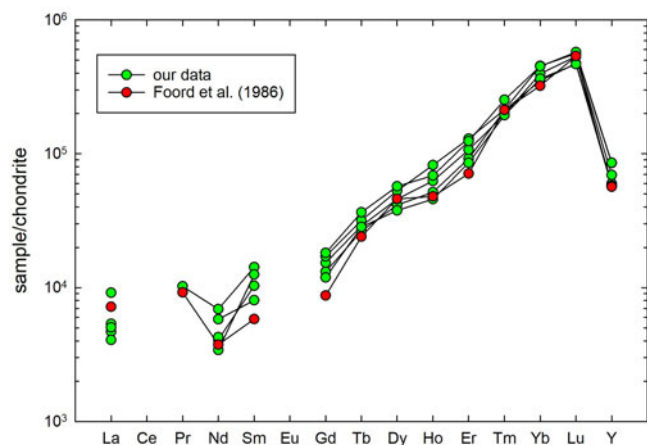


Figure 3. Comparison of REE patterns of 'gadolinites' from Jaguarçu pegmatite with those of Foord *et al.* (1986).

of hingganite-(Nd) (Kasatkin *et al.*, 2020) and -(Y) (Gorelova *et al.*, 2020) have similar intensities in all the range (except the OH region). However, the differences in the intensity of Raman bands can be attributed to the crystal orientation effects.

Crystal structure of Bi-rich 'gadolinites' from the Jaguarçu Pegmatite at ambient temperature

Both crystals of 'minasgeraisite-(Y)' under study demonstrate the typical features of 'gadolinites' and do not have significant differences (Table 1, Supplementary Tables S1, S2, and the crystallographic information files (cif) which have been deposited with the Principal Editor of *Mineralogical Magazine* and are available with Supplementary material, see below). Unfortunately, it was not possible for us to check the lowering symmetry in 'minasgeraisite-(Y)' due to the installed thermal plant and the relatively low quality of the crystals available.

The unit cell parameters of 'minasgeraisite-(Y)' studied by us are close to those obtained by Cooper and Hawthorne (2018),

but higher than those reported by Foord *et al.* (1986). It is worth noting that Foord *et al.* (1986) obtained the unit cell parameters from powder XRD data, so their measurement is inimitable because it is impossible to get a similar ratio of REE and Bi due to the strong zoning. The bismuth content in 'gadolinites' from the Jaguarçu Pegmatite varies from ~8 to ~28 wt.% Bi₂O₃ (Table 1). An increase in bismuth content is accompanied by yttrium content decrease. This means that the Bi-rich zone would have higher unit-cell parameters compared to the Y-rich zone as the Bi ionic radius is higher than that of Y (^[VIII]r_{Bi} = 1.02, ^[VIII]r_Y = 1.17 Å; Shannon, 1976).

The data obtained on the geometry of the main polyhedra (Supplementary Table S2) clearly indicate the similarities between both our crystals of 'minasgeraisite-(Y)' and the crystal of 'minasgeraisite-(Y)' studied by Cooper and Hawthorne (2018). The mean <A–O> distance varies from 2.436 to 2.504 Å, which is close to the value in the crystal structure of gadolinite-(Nd) (2.496 Å; Škoda *et al.*, 2018). Our data match the observation of Cooper and Hawthorne (2018) who discovered that the low site-scattering at the M-site precludes the possibility of the M site to be Ca-dominant in 'minasgeraisite-(Y)'. The mean <M–O> distance in the crystal structure of 'minasgeraisite-(Y)' (according to both our data and those of Cooper and Hawthorne (2018)) varies from 2.177 to 2.188 Å and falls within the range 2.151–2.200 Å reported for other 'gadolinites' with a variable Fe/Mg/Mn occupancy at the M site (Demartin *et al.*, 2001; Gorelova *et al.*, 2020). Interestingly, our observations indicate a necessary role of Mn (Tables 1, 3) besides the vacancy which dominates at the M site. Synthetic 'gadolinite' with the composition Y₂MnBe₂Si₂O₈O₂ has already been reported (Ito, 1965). This means that Mn could be the main cation at the M site and that Mn-dominant 'gadolinites' could be found in Nature. We think that detailed data on the crystal structure of synthetic 'gadolinites' should solve the issue relating to the M site occupancies by various cations. To date, only information on the crystal structure of Yb₂NiBe₂Si₂O₈O₂ (Foit and Gibbs, 1975) is available, though 'gadolinites' with various A- and M-site compositions (e.g. Gd₂CdBe₂Si₂O₈O₂) have been synthesised (Ito, 1965) they have

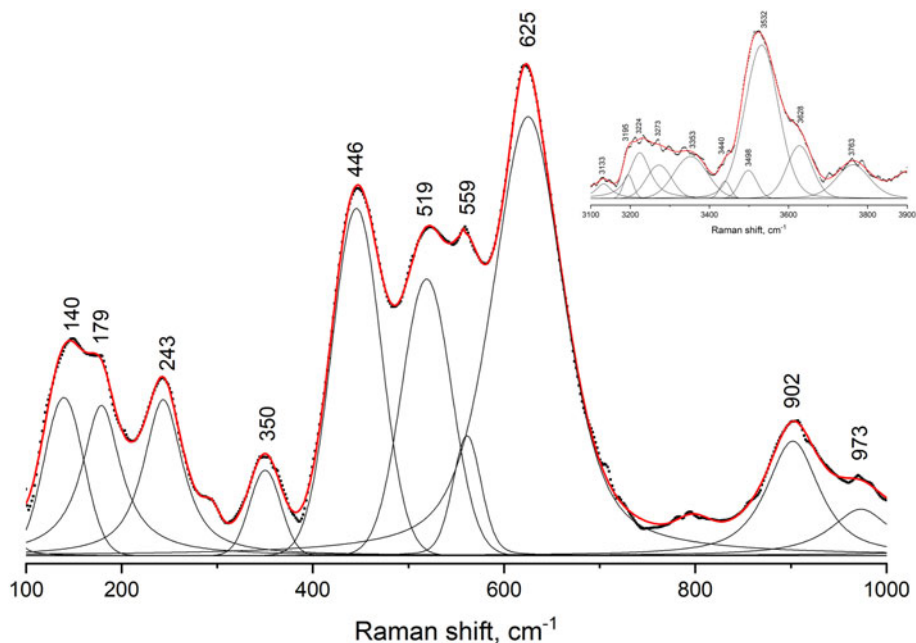


Figure 4. Raman spectrum of 'minasgeraisite-(Y)'. The black line shows the experimental data, the grey line shows the peak deconvolution and the red line shows the calculated spectra.

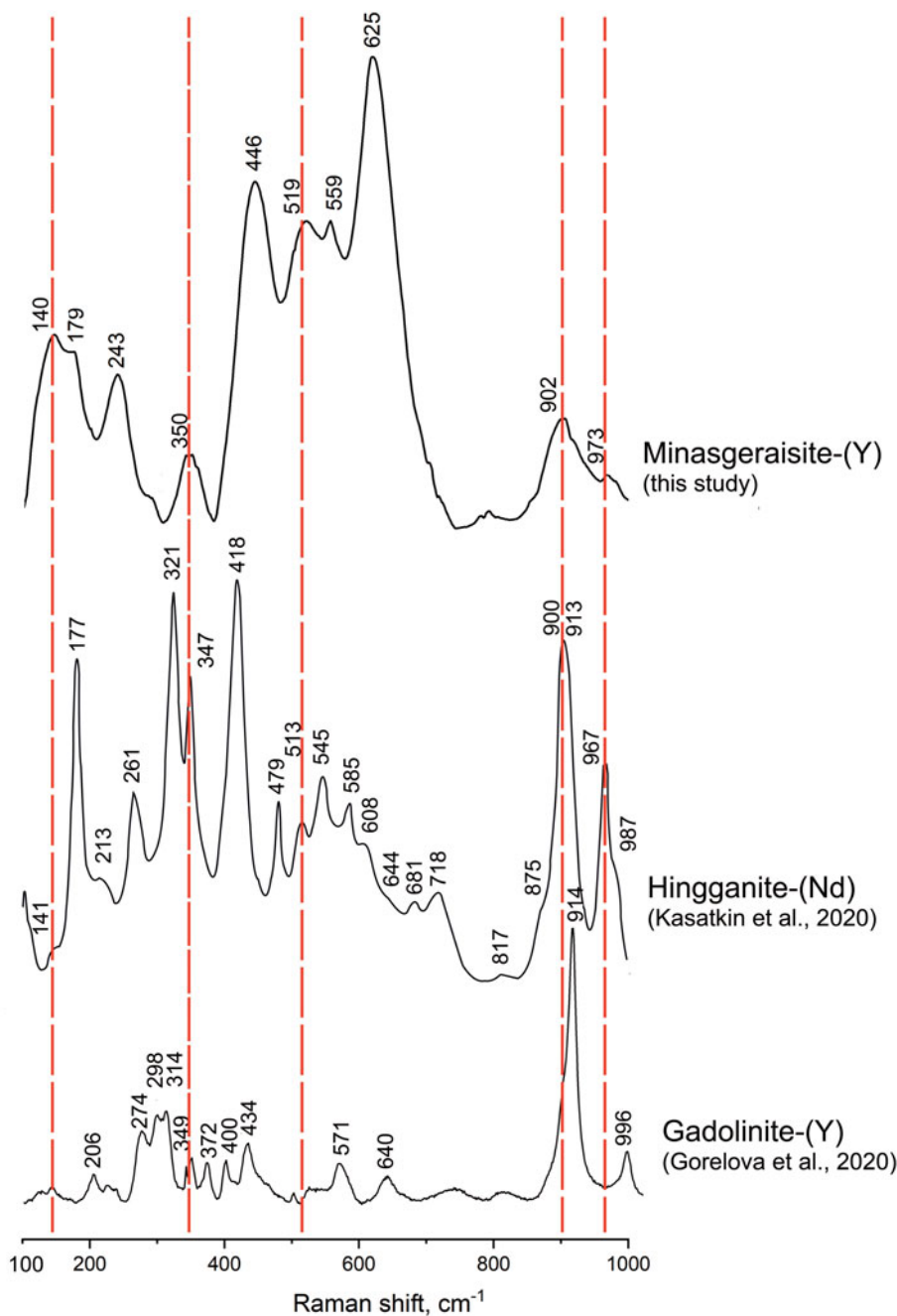


Figure 5. Comparison of Raman spectra of gadolinite-subgroup minerals from this work with Kasatkin *et al.* (2020) and Gorelova *et al.* (2020).

not been studied in detail. As the cadmium ionic radius is very close to that of calcium ($^{[VI]}r_{\text{Cd}} = 0.95$, $^{[VI]}r_{\text{Ca}} = 1.00$ Å; Shannon, 1976) but much greater than the ionic radius of Fe^{2+} or Ni ($^{[VI]}r_{\text{Ni}} = 0.78$; $^{[VI]}r_{\text{Ni}} = 0.69$ Å; Shannon, 1976), it should be possible to check the interatomic distances and prove such an option (the *M* site occupied by a relatively large cation) in general.

According to our data and those of Cooper and Hawthorne (2018), the *Q* site demonstrates mixed occupancies, while the *T* site is fully occupied by Si. The mean $\langle T\text{-O} \rangle$ distances (1.625–1.631 Å) are typical for $\langle \text{Si-O} \rangle$ distances in the tetrahedra of ‘gadolinites’ (e.g. Demartin *et al.*, 2001; Gorelova *et al.*, 2020). Interestingly, the data on ‘minasgeraisite-(Y)’ show the presence of both Be and Si at the *Q* site, which is evident from the site scattering and the mean $\langle Q\text{-O} \rangle$ distances (1.610–1.632 Å).

Previously, Demartin *et al.* (2001) hesitated as to whether Si could occupy the *Q* site, however both the elemental composition and the crystal-structure refinement confirm Be for Si substitution (Table 1, 3) and are in agreement with the data of Allaz *et al.* (2020). This observation indicates that the normalisation of the chemical formula of gadolinite-group minerals assuming Si = 2 apfu can generate false vacancies at the *A* and *M* sites and unbalance the OH–O occupation at the φ site.

The *A* site of gadolinite-group minerals can adopt relatively large cations with variable ionic radius: Ca = 1.12 Å, light $\text{Ln}^{3+} = 1.16\text{--}1.10$ Å, heavy $\text{Ln}^{3+} = 1.03\text{--}0.98$ Å and Y = 1.11 Å. The ionic radius of Bi^{3+} is 1.17 Å, which is very close to La^{3+} . Due to the same charge of Bi and REE and similar ionic radii, Bi should fit well into the gadolinite structure, however, Bi is not a common element in gadolinite-group minerals. Its elevated

Table 2. Main Raman bands (cm⁻¹) in gadolinite-subgroup minerals.

Range, cm ⁻¹	'Minasgeraisite-(Y)'	Hingganite-(Y)	Hingganite-(Nd)	Gadolinite-(Y)	Gadolinite-(Nd)
100–300	140, 179, 243	116, 186, 268	97, 141, 177, 213, 261, 274	206, 274, 298	104, 143, 203, 225, 265, 292
300–450	350, 446	328, 423	321, 347, 418	314, 349, 372, 400, 434	306, 309, 363, 383, 411, 428
450–650	519, 559	541, 584	479, 513, 545, 585, 608	571, 640	483, 501, 550, 615
650–750	625	725	681, 718	~730	677, 707
750–850			817	~820	~800
850–1000	902, 973	923, 983	875, 900, 913, 967, 987	914, 996	897, 970
3200–4000	3224, 3353, 3532, 3763	3383, 3541		3462, 3477, 3543	3525
Reference	This work	Gorelova <i>et al.</i> (2020)	Kasatkin <i>et al.</i> (2020)	Gorelova <i>et al.</i> (2021a)	Škoda <i>et al.</i> (2018)

content has only been reported from the Jaguarçu pegmatite. The mineral under investigation exhibits a characteristic heavy-REE-enriched pattern (Fig. 3), nevertheless it contains a high content of large ions (Ca and Bi). Therefore, the <A–O> distance of minasgeraisite-(Y) is similar to that of gadolinite-(Nd) (Škoda *et al.*, 2018) due to the similarities in ionic radius for Bi and Ce with a light REE.

Minasgeraisite-(Y) probably crystallised from the late hydrothermal fluids enriched in heavy Ln³⁺, Ca, Bi, B, Be and Mn, but poor in Fe²⁺. The presence of late churchite-(Y), chernovite-(Y), agakhanovite-(Y) and the absence of Ce-dominant secondary minerals in the Jaguarçu pegmatite testify for the heavy-REE-enriched character of the hydrothermal fluids. The heavy REE can be sourced from an alteration of an early formed magmatic heavy-REE mineral (euxenite-(Y)?). The absence of Fe and Ce in minasgeraisite could indicate an elevated *f*_{O₂} in the fluids; Ce³⁺ oxidised to Ce⁴⁺, which precipitated before the formation of minasgeraisite-(Y) and Fe²⁺ oxidised to Fe³⁺, which rarely concentrates in gadolinite-group minerals.

High-temperature behaviour of 'minasgeraisite-(Y)' and other gadolinite-group minerals

Temperature dependencies for the unit-cell parameters of 'minasgeraisite-(Y)' are shown in Fig. 6. Below 900°C all unit-cell parameters undergo continuous expansion, whereas above this temperature, all but *c* start to decrease. These changes indicate the beginning of the decomposition of 'minasgeraisite-(Y)' that is also confirmed by a significant deterioration in quality of SCXRD data (Table S1).

There are only seven experimental points for the calculations of thermal expansion coefficients (TECs) as 'minasgeraisite-(Y)' starts to decompose at the last two temperatures. Taking this fact into account, the TECs were calculated only with the linear approximation and are the following: α₁₁ = 7.0(5), α₃₃ = 3.0(6), μ(α₃₃^c) = 31.5(4), α_a = 5.9(5), α_b = α₂₂ = 10.2(5), α_c = 4.1(6), α_β = 2.2(4), α_V = 20.2(9) × 10⁶ °C⁻¹. The results we obtained demonstrate that the thermal expansion of 'minasgeraisite-(Y)' has quite an anisotropic character (α_{max} / α_{min} = 3.4), wherein the maximum and minimum expansions are close to the *b* and *c* directions, respectively,

Table 3. Miscellaneous crystallographic data for 'gadolinites'.

	'Minasgeraisite-(Y)'	Minasgeraisite-(Y)	Hingganite-(Y)	Gadolinite-(Y)	Gadolinite-(Nd)		
<i>a</i> (Å)	4.7560(4)	4.7476(4)	4.764(2)*	4.702(1)*	4.7494(3)	4.7136(4)	4.8216(3)
<i>b</i> (Å)	7.6721(5)	7.6586(5)	7.705(3)	7.562(1)	7.6003(3)	7.5180(8)	7.6985(4)
<i>c</i> (Å)	9.9678(7)	9.9467(9)	9.994(4)*	9.833(2)*	9.8794(3)	9.8724(8)	10.1362(6)
α (°)	90	90	90.042(9)	90	90	90	90
β (°)	90.265(7)	90.230(7)	90.218(14)	90.46(6)	90.304(4)	89.573(7)	90.234(4)
γ (°)	90	90	90.034(9)	90	90	90	90
<i>V</i> (Å ³)	363.71(5)	361.66(5)	366.8(5)	349.60(14)	356.61(3)	349.84(6)	376.24(6)
Space group	<i>P</i> ₂ / <i>c</i>	<i>P</i> ₂ / <i>c</i>	<i>P</i> ₁	<i>P</i> ₂ / <i>a</i>	<i>P</i> ₂ / <i>c</i>	<i>P</i> ₂ / <i>c</i>	<i>P</i> ₂ / <i>c</i>
<i>Z</i>	2	2	1	2	2	2	2
Radiation	MoKα	MoKα	MoKα	CuKα	MoKα	MoKα	MoKα
No. of reflections	3555	3528	13109	2018	1270	2955	2955
No. unique reflections	872	894	4288	1113	617	875	875
No. of observed reflections	752	782	4170	985	566	607	607
	[<i>I</i> > 2σ(<i>I</i>)]	[<i>I</i> > 2σ(<i>I</i>)]	[<i>I</i> > 2σ(<i>I</i>)]	[<i>I</i> > 2σ(<i>I</i>)]	[<i>I</i> > 2σ(<i>I</i>)]	[<i>I</i> > 2σ(<i>I</i>)]	[<i>I</i> > 3σ(<i>I</i>)]
<i>R</i> ₁ (%)	6.3	7.9	2.86	4.8	5.3	3.7	3.7
<i>wR</i> ₂ (%)	12.6	16.7	7.08	10.5	14.0	7.8	7.8
<A–O>	2.421	2.417	2.436–2.504	2.440	2.413	2.496	2.496
A-site composition	Y _{1.80} Bi _{0.20}	Y _{1.70} Bi _{0.30}	Y _{0.71} Ca _{0.60} Bi _{0.40} Er _{0.29} **	Y _{0.72} Ca _{0.56} Ln _{0.41} Bi _{0.31}	Y ₂	Y _{1.68} Yb _{0.32}	Nd _{1.942}
<M–O>	2.183	2.177	2.177–2.188	2.190	2.151	2.190	2.190
M-site composition	□ _{0.88} Mn _{0.12}	□ _{0.75} Mn _{0.25}	□ _{0.69} Mn _{0.41} **	Ca _{0.45} Mn _{0.20} □ _{0.19} Mg _{0.08} × Fe _{0.05} Zn _{0.02} Cu _{0.01}	□ _{0.66} Fe _{0.34}	Fe _{0.85} □ _{0.15}	Fe _{1.00}
<T–O>	1.630	1.625	1.628–1.632	1.626	1.618	1.646	1.646
T-site composition	Si ₂	Si ₂	Si ₂ **	Si _{1.95} P _{0.08}	Si ₂	Si ₂	Si _{1.96} Be _{0.04}
<Q–O>	1.612	1.614	1.610–1.632	1.595	1.620	1.635	1.635
Q-site composition	Be _{1.76} Si _{0.24}	Be _{1.8} Si _{0.2}	Be _{1.66} B _{0.20} Si _{0.14} **	Be _{1.55} B _{0.21} Si _{0.24}	Be ₂	Be ₂	Be _{1.95} Si _{0.05}
Reference	Our data, crystal 1	Our data, crystal 2	Cooper and Hawthorne (2018)	Foord <i>et al.</i> (1986)	Gorelova <i>et al.</i> (2020)	Gorelova <i>et al.</i> (2021a)	Škoda <i>et al.</i> (2018)

Note: * *a* and *c* parameters were transformed for comparison, ** A-, M-, Q- and T-site compositions are averaged for comparison.

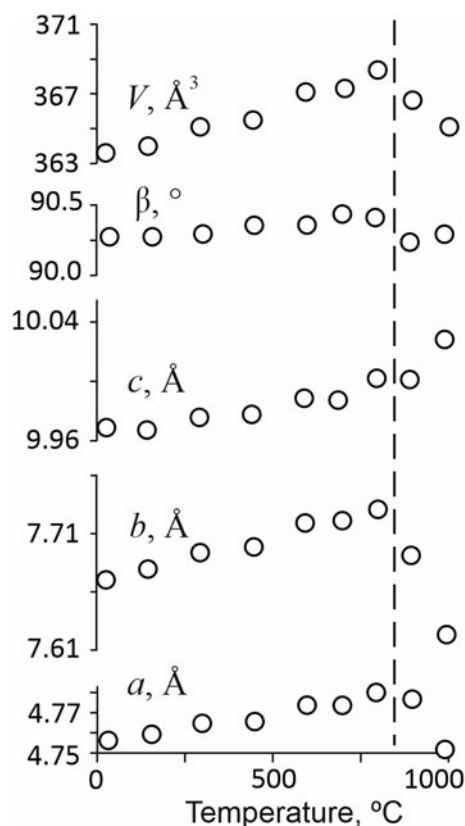


Figure 6. The unit-cell parameters of 'minasgeraisite-(Y)' at different temperatures. The errors are smaller than symbols. The broken line demonstrates the start of decomposition process.

i.e. within the layer plane (Fig. 7). Generally, such a type of high-temperature deformations is not typical for layered crystal structures, which typically expand more intensely perpendicular to the layer plane; however, it has been observed previously for other gadolinite-supergroup minerals (Krzhizhanovskaya *et al.*, 2018; Gorelova *et al.*, 2020; 2021a; 2022) and is usually explained by the shear deformation of the monoclinic plane (Bubnova and Filatov, 2008).

The volume thermal expansion of 'minasgeraisite-(Y)' is quite low ($\alpha_V = 20 \times 10^{-6} \text{ }^\circ\text{C}^{-1}$) in comparison with the other gadolinite-supergroup minerals. Hingganite-(Y), which is the closest in composition to 'minasgeraisite-(Y)' studied here, has an even lower volume TEC ($\alpha_V = 9 \times 10^{-6} \text{ }^\circ\text{C}^{-1}$; Gorelova *et al.*, 2020), but such a comparison is not totally correct, as hingganite-(Y) was only studied at low temperatures (from -173 to $+7^\circ\text{C}$). The third mineral of the gadolinite subgroup, namely gadolinite-(Y), expands at high temperatures one and a half times more intensely ($\alpha_V = 28 \times 10^{-6} \text{ }^\circ\text{C}^{-1}$; Gorelova *et al.*, 2021a) than 'minasgeraisite-(Y)'. It should also be noted that if gadolinite-(Y) starts to decompose at the temperature above 1050°C (Gorelova *et al.*, 2021a), 'minasgeraisite-(Y)' is less stable and starts to decompose above 800°C .

The results obtained throughout this study imply that beryll-silicate compounds of the gadolinite-supergroup minerals are the most stable compared to borosilicate and beryllphosphate analogues. Datolite, 'bakerite' and hydroxylherderite, from previous studies (Krzhizhanovskaya *et al.*, 2018; Gorelova *et al.*, 2022), start to decompose at 710 , 530 and 720°C , respectively. It is interesting to note that though the high-temperature and high-pressure behaviour have to be similar (antipodal) (Hazen, Finger, 1982; Filatov, 1990), according to the general principles of comparative crystal chemistry, beryllphosphates are usually more stable compared to beryll-, boro- and aluminosilicate

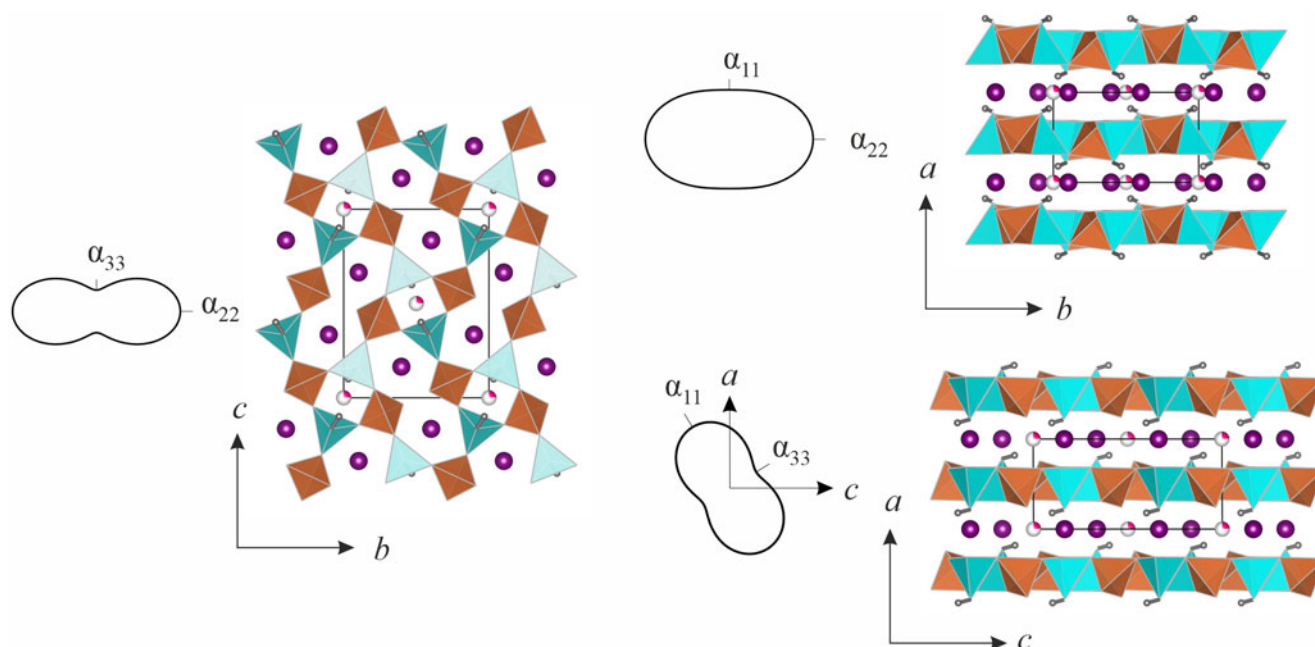


Figure 7. Crystal structure of 'minasgeraisite-(Y)' with the section of the averaged thermal expansion. SiO_4 and BeO_4 tetrahedra are given in orange and blue, respectively. Atoms of A site and H atoms are shown as purple and grey spheres, respectively, whereas atoms of M site are shown as white and rose that demonstrates the partial occupancy.

compounds under high-pressure conditions (Gorelova *et al.*, 2021b; Gorelova *et al.*, 2022). This difference in the high-temperature and high-pressure behaviour can be explained by the different (OH)-content in the minerals of the gadolinite supergroup. The decomposition at the temperature at $\sim 700^\circ\text{C}$ is typical for (OH)-containing layered minerals and inorganic compounds (e.g. Foeldvari, 2011), whereas (OH) groups do not have such a strong influence on the high-pressure behaviour. It is also worth noting that our data are in line with the previous observations on synthetic 'gadolinites' of Ito (1965), who stated that they are stable from 300 to 1200°C .

Conclusion

Minasgeraisite-(Y) is a mineral, whose description lacks structural data but contains information on the presence of a large cation (Ca) at the *M* site, which is atypical for 'gadolinites'. Several scientists hesitated about the existence of minasgeraisite-(Y), however due to its rarity in Nature, it has still not been possible to re-investigate minasgeraisite-(Y) or (at least) to reinvestigate 'gadolinite' from the minasgeraisite-(Y) type locality.

Our study revealed a significant similarity between the composition of 'minasgeraisite-(Y)' studied by us and that of minasgeraisite-(Y) discovered by Foord *et al.* (1986). 'Minasgeraisite-(Y)' studied by us has high Bi and Mn content, which is typical for minasgeraisite-(Y) (Foord *et al.*, 1986) and has not been encountered in any other 'gadolinite' localities. Generally, the sample under investigation has all the specific features of the chemical composition of minasgeraisite-(Y) from the Jaguaraçu Pegmatite, except Ca excess at the *M* site, which implies that it should rather be considered as Bi-rich, Mn-bearing hingganite-(Y) than minasgeraisite-(Y).

Our study also revealed a considerable similarity between the crystal structure of 'minasgeraisite-(Y)' studied by us and that of 'minasgeraisite-(Y)' studied by Cooper and Hawthorne (2018). We have found that the geometry and occupancies of all non-equivalent sites in the crystal structure of 'minasgeraisite-(Y)' studied by us are consistent with those in the crystal structure of 'minasgeraisite-(Y)' studied by Cooper and Hawthorne (2018). Our data match the observation of Cooper and Hawthorne (2018), that the low site-scattering at the *M* site precludes the possibility of the *M* site to be Ca-dominant in 'minasgeraisite-(Y)'. However, it is worth noting that we did not observe the lowering of the symmetry of the crystal under investigation (probably due to the relatively low quality and low amount of the data available).

'Minasgeraisite-(Y)' (Bi-rich, Mn-bearing hingganite-(Y)) studied by us starts to decompose above 800°C , which shows that it is more stable than borosilicate and beryllophosphate analogues ($< 720^\circ\text{C}$; Krzhizhanovskaya *et al.*, 2018; Gorelova *et al.*, 2022) but less stable than another beryllosilicate analogue with the fully occupied *M* site ($\sim 1050^\circ\text{C}$; Gorelova *et al.*, 2021a). We can conclude that beryllosilicates are most stable at high-temperature conditions within the gadolinite supergroup and that the species with a higher *M*-site occupancy have higher stability upon heating.

Acknowledgements. The authors thank the X-ray Diffraction Centre and Geomodel Center of the Resource Centre of Saint Petersburg State University for providing instrumental and computational resources. We are thankful to Principal Editor Dr. S. Mills for editorial handling of the manuscript and to the Structures Editor for corrections of crystallographic data. The constructive suggestions and invaluable linguistic support of two anonymous reviewers are gratefully acknowledged. This research was funded by the Russian Science Foundation, grant number 22-27-00430.

Supplementary material. The supplementary material for this article can be found at <https://doi.org/10.1180/mgm.2023.19>.

Competing interests. The authors declare none.

References

- Agilent (2012) *CrysAlisPRO*. Agilent Technologies Ltd, Yarnton, Oxfordshire, England.
- Allaz J.M., Smyth J.R., Henry R.E., Stern C.R., Persson P., Ma J.J. and Raschke M.B. (2020) Beryllium-silicon disorder and rare earth crystal chemistry in gadolinite from the White Cloud pegmatite, Colorado, USA. *The Canadian Mineralogist*, **58**, 829–845.
- Bačík P., Fridrichová J., Uher P., Pršek, J. and Ondrejka M. (2014) The crystal chemistry of gadolinite-datolite group silicates. *The Canadian Mineralogist*, **52**, 625–642.
- Bačík P., Miyawaki R., Atencio D., Camara F. and Fridrichová J. (2017) Nomenclature of gadolinite supergroup. *European Journal of Mineralogy*, **29**, 1067–1082.
- Belolipetsky A.P., Pletneva N.I., Denisov A.P. and Kulchitskaya E.A. (1968) Accessory gadolinites from pegmatites and granite veins on Kola Peninsula. Pp. 162–173 in: *Mineralogical Materials of Kola Peninsula* (I. V. Belkov, editor), Vol. 6. Nauka, Leningrad, Russia [in Russian].
- Bubnova R.S. and Filatov S.K. (2008) Strong anisotropic thermal expansion in borates. *Physica Status Solidi*, **245**, 2469–2476.
- Bubnova R.S., Firsova V.A. and Filatov S.K. (2013) Software for determining the thermal expansion tensor and the graphic representation of its characteristic surface (Theta to Tensor-TTT). *Glass Physics and Chemistry*, **39**, 347–350.
- Cooper M.A. and Hawthorne F.C. (2018) Cation order in the crystal structure of 'minasgeraisite-(Y)'. *Mineralogical Magazine*, **82**, 301–312.
- Cooper M.A., Hawthorne F.C., Miyawaki R. and Kristiansen R. (2019) Cation order in the crystal structure of 'Ca-hingganite-(Y)'. *The Canadian Mineralogist*, **57**, 371–382.
- Demartin F., Pilati T., Diella V., Gentile P. and Gramaccioli C.M. (1993) A crystal-chemical investigation of Alpine gadolinite. *The Canadian Mineralogist*, **30**, 127–136.
- Demartin F., Minaglia A. and Gramaccioli C.M. (2001) Characterization of gadolinite-group minerals using crystallographic data only: the case of hingganite-(Y) from Cuasso al Monte, Italy. *The Canadian Mineralogist*, **39**, 1105–1114.
- Filatov S.K. (1990) *High Temperature Crystal Chemistry*. Nedra, Leningrad, Russia, 288 pp. [in Russian].
- Foit F.F. and Gibbs G.V. (1975) Refinement of $\text{NiYb}_2\text{Be}_2\text{Si}_2\text{O}_{10}$, a gadolinite-type structure. *Zeitschrift für Kristallographie*, **141**, 375–386.
- Földvári M. (2011) *Handbook of Thermogravimetric System of Minerals and Its Use in Geological Practice*. Geological Institute of Hungary, Budapest, Hungary, 180 pp.
- Foord E.E., Gaines R.V., Crock J.G., Simmons W.B. and Barbosa C.P. (1986) Minasgeraisite, a new member of the gadolinite group from Minas Gerais, Brazil. *American Mineralogist*, **71**, 603–607.
- Gibson S.J. and Ehlmann A.J. (1970) Annealing characteristics of metamict gadolinite from Rode Ranch Texas. *American Mineralogist*, **55**, pp. 288–291.
- Gorelova L.A., Vereshchagin O.S., Cuchet S., Shilovskikh V. and Pankin D. (2020) Low-Temperature Crystal Chemistry of Hingganite-(Y), from the Wann Glacier, Switzerland. *Minerals*, **10**(322), 1–16.
- Gorelova L.A., Panikorovskii T.L., Pautov L.A., Vereshchagin O.S., Krzhizhanovskaya M.G. and Spiridonova D.V. (2021a) Temperature-versus compositional-induced structural deformations of gadolinite group minerals with various Be/B ratio. *Journal of Solid State Chemistry*, **299**, 1–12.
- Gorelova L.A., Pakhomova A.S., Krzhizhanovskaya M.G., Pankin D.V., Krivovichev S.G., Dubrovinsky L.S. and Kasatkin A.V. (2021b) Crystal structure evolution of slawsonite $\text{SrAl}_2\text{Si}_2\text{O}_8$ and paracelsian $\text{BaAl}_2\text{Si}_2\text{O}_8$ upon compression and decompression. *The Journal of Physical Chemistry C*, **125**, 13014–13023.
- Gorelova L.A., Vereshchagin O.S., Aslandukov A., Aslandukova A., Spiridonova D.V., Krzhizhanovskaya M.G., Kasatkin A.V. and

- Dubrovinsky L.S. (2022) Hydroxylherderite ($\text{Ca}_2\text{Be}_2\text{P}_2\text{O}_8(\text{OH})_2$) stability under extreme conditions (up to 750 °C / 100 GPa). *Journal of the American Ceramic Society*, **106**, <https://doi.org/10.1111/jace.18923>.
- Grew E. S. and Hazen R.M. (2014) Beryllium mineral evolution. *American Mineralogist*, **99**, 999–1021.
- Habel A. and Habel M. (2009) Minasgeraisit-(Y) aus dem Krennbruch in Matzersdorf/Tittling. *Mineralien-Welt*, **20**(5), 51–53 [in German].
- Hazen R.M. and Finger L.W. (1982) *Comparative Crystal Chemistry: Temperature, Pressure, Composition and the Variation of Crystal Structure*. John Wiley and Sons Ltd.: London, UK, 231 pp.
- Ito J. (1965) The synthesis of gadolinite. *Proceedings of the Japan Academy*, **41**, 404–407.
- Ito J. (1966) A note on gadolinite synthesis. *Proceedings of the Japan Academy*, **42**, 634–635.
- Ito J. (1967) Synthesis of calciogadolinite. *American Mineralogist*, **52**, 1523–1527.
- Ito J. and Hafner S.S. (1974) Synthesis and study of gadolinites. *American Mineralogist*, **59**, 700–708.
- Kasatkin A.V., Nestola F., Škoda R., Chukanov N.V., Agakhanov A.A., Belakovskiy D.I., Lanza A., Holá M. and Rumsey M.S. (2020) Hingganite-(Nd), $\text{Nd}_2\text{Be}_2\text{Si}_2\text{O}_8(\text{OH})_2$, a new gadolinite-super group mineral from Zagi Mountain, Pakistan. *The Canadian Mineralogist*, **58**, 549–562.
- Krzyszhanovskaya, M.G., Gorelova, L.A., Bubnova, R.S. Pekov I.V. and Krivovichev S.V. (2018) High-temperature crystal chemistry of layered calcium borosilicates: $\text{CaBSiO}_4(\text{OH})$ (datolite), $\text{Ca}_4\text{B}_5\text{Si}_3\text{O}_{15}(\text{OH})_5$ ('bakerite') and $\text{Ca}_2\text{B}_2\text{SiO}_7$ (synthetic analogue of okayamalite). *Physics and Chemistry of Minerals*, **45**, 463–473.
- Lyalina L.M., Selivanova E.A., Savchenko Y.E., Zozulya D.R. and Kadyrova G.I. (2014) Minerals of the gadolinite-(Y)-hingganite-(Y) series in the alkali granite pegmatites of the Kola Peninsula. *Geology of Ore Deposits*, **56**, 675–684. <https://doi.org/10.1134/S1075701514080042>.
- Malczewski D. and Janeczek J. (2002) Activation energy of annealed metamict gadolinite from ^{57}Fe Moessbauer spectroscopy. *Physics and Chemistry of Minerals*, **29**, 226–232.
- Merlet C. (1994) An accurate computer correction program for quantitative electron probe microanalysis. *Microchimica Acta*, **114/115**, 363–376.
- Novák M., Kadlec T. and Gadas P. (2013) Geological position, mineral assemblages and contamination of granitic pegmatites in the Moldanubian Zone, Czech Republic; examples from the Vlastějovice region. *Journal of Geosciences*, **58**(1), 21–47.
- Paulmann C., Zietlow P., McCammon C., Salje E.K.H. and Bismayer U. (2019) Annealing of metamict gadolinite-(Y): X-ray diffraction, Raman, IR, and Moessbauer spectroscopy. *Zeitschrift für Kristallographie*, **234**, 587–593.
- Shannon R.D. (1976) Revised effective ionic radii and systematic studies of interatomic distances in halides and chalcogenides. *Acta Crystallographica*, **A32**, 751–767.
- Sheldrick G.M. (2015) Shelxt – integrated space-group and crystal-structure determination. *Acta Crystallographica*, **A71** 3–8.
- Škoda R., Plášil J., Jonsson E., Čopjaková R., Langhof J. and Galiová M.V. (2015) Redefinition of thalénite-(Y) and discreditation of fluorthalénite-(Y): A re-investigation of type material from the Österby pegmatite, Dalarna, Sweden, and from additional localities. *Mineralogical Magazine*, **79**, 965–983.
- Škoda R., Plášil J., Čopjaková R., Novák M., Jonsson E., Galiová M. V. and Holtstam D. (2018) Gadolinite-(Nd), a new member of the gadolinite supergroup from the Fe-REE deposits of Bastnas-type, Sweden. *Mineralogical Magazine*, **82**, 133–145.
- Voloshin A.V., Pakhomovsky Ya.A. and Sorokhtina N.V. (2002) Compositions of minerals from gadolinite group in amazonite and pegmatites of Kola Peninsula. *Vestnik MGTU*, **5**, 61–70.
- Zajzon N., Szakáll S., Kristály F., Váczi T. and Fehér B. (2015) Gadolinite-bearing NYF-type pegmatite from Sukoró, Velence Hills, Hungary. *Acta Mineralogica-Petrographica*, **9**, 75.